Applied Physics Letters

Light-matter interaction in open cavities with dielectric stacks

Cite as: Appl. Phys. Lett. **118**, 154002 (2021); https://doi.org/10.1063/5.0047145
Submitted: 10 February 2021 • Accepted: 20 March 2021 • Published Online: 12 April 2021

Astghik Saharyan, Juan-Rafael Álvarez, Thomas H. Doherty, et al.

Applied Physics Letters ARTICLE scitation.org/journal/apl

Light-matter interaction in open cavities with dielectric stacks

Cite as: Appl. Phys. Lett. **118**, 154002 (2021); doi: 10.1063/5.0047145
Submitted: 10 February 2021 · Accepted: 20 March 2021 ·
Published Online: 12 April 2021

Astghik Saharyan,[1] Juan-Rafael Álvarez,[2] Thomas H. Doherty,[2] Axel Kuhn,[2,a)] and Stéphane Guérin[1,a)]

AFFILIATIONS

[1]Laboratoire Interdisciplinaire Carnot de Bourgogne, CNRS UMR 6303, Université Bourgogne Franche-Comté, BP 47870, F-21078 Dijon, France
[2]Clarendon Laboratory, University of Oxford, Parks Road, Oxford OX1 3PU, United Kingdom

Note: This paper is part of the APL Special Collection on Non-Classical Light Emitters and Single-Photon Detectors.
[a)]**Authors to whom correspondence should be addressed:** axel.kuhn@physics.ox.ac.uk and sguerin@u-bourgogne.fr

ABSTRACT

We evaluate the exact dipole coupling strength between a single emitter and the radiation field within an optical cavity, taking into account the effects of multilayer dielectric mirrors. Our model allows one to freely vary the resonance frequency of the cavity, the frequency of light or atomic transition addressing it, and the design wavelength of the dielectric mirror. The coupling strength is derived for an open system with unbound frequency modes. For very short cavities, the effective length used to determine their mode volume and the lengths defining their resonances are different, and also found to diverge appreciably from their geometric length, with the radiation field being strongest within the dielectric mirror itself. Only for cavities much longer than their resonant wavelength does the mode volume asymptotically approach that normally assumed from their geometric length.

The development of universal quantum computation remains a key endeavor in the coherent control and manipulation of light and matter quantum states. A principal component of this effort is improving the inherent scalability of current architectures and developing methods for the reliable interconnection of distant qubits and quantum processors.[1] A promising approach is the use of high finesse optical cavities to couple individual states of light and matter, connecting stationary emitters and traveling photons as the hosts of quantum information. A strong coupling within the cavity allows this to be a controllable, deterministic, and inherently reversible interaction, essentially establishing an idealized quantum interface.[2,3] In principle, this allows for the generation of light-matter entanglement,[4] entanglement swapping,[5] and the distribution of cluster states over an extended quantum network.[6] Similar systems have been used extensively for the enhanced production of single photons, across a variety of emitter types and platforms such as neutral atoms,[7] ions,[8] NV centers,[9] and quantum dots.[10]

The Purcell effect plays an important role in the realization of cavity mediated light-matter coupling schemes. It describes the enhancement to the spontaneous emission rate of a quantized emitter within a resonant cavity. When compared to spontaneous emission into free space, the rate of emission into the cavity mode for an atom localized at the field maximum is enhanced by[11] $F_p = 3\lambda^3 Q/4\pi^2 V$, where Q is the quality factor of the resonator, λ is the transition wavelength, and V is the optical mode volume of the resonator. In cavity QED systems which only couple to a single emitter, this factor is expressed as system cooperativity, given by $2C = F_p = g^2/(\kappa\gamma)$, where g is the atom-cavity coupling rate, κ is the cavity field decay rate, and 2γ is the rate of atomic spontaneous emission. Strongly coupled systems are correspondingly defined as those where $g \gg (\kappa, \gamma)$, i.e., where the coherent coupling rate surpasses incoherent decay mechanisms.[12] The suppression of photonic decay within the cavity generally requires the use of highly reflective mirrors, characterized by a large cavity finesse,[13] $\mathscr{F} = \pi\sqrt{R}/(1-R)$, where R is the mirror reflectivity. Given the equivalent representation of finesse as the ratio of cavity free spectral range to its linewidth, a high finesse ensures that an emitter couples to a single cavity resonant mode.

To achieve the mirror reflectivity required for coherent atom-cavity interactions, highly reflective dielectric coatings or Bragg stacks are used as standard.[14] These comprise layer pairs of quarter-wavelength optical thickness dielectric material, with alternating refractive indices. Generally, a high reflectivity is only achieved for a

large number of such layers, implying a notable penetration of the stack by incident light. A common strategy for enhancing cooperativity is the minimization of mode volume, which generally requires reducing mirror spacing. At its extreme, the mirror spacing can be of the same order as the resonant wavelength of interest.[15] This unintentionally increases the relative portion of the cavity mode within the dielectric stack,[14,16,17] rendering inaccurate the standard spectral properties of a Fabry–Pérot resonator such as its resonance frequency, linewidth, and free spectral range. The propagation of light in cavities limited by dielectric mirrors has been studied under the resonance condition, where the frequency of the light matches a resonance frequency of the Fabry–Pérot cavity as well as the design frequency of the mirror stack.[14,17,18] Additionally, this problem has also been studied numerically for calculating the mode volume of leaky optical cavities.[19–21] Here, we go a step further in considering the more general case of a wave of arbitrary wavelength traveling through the stack: This is always the case if the emitter coupled to the cavity is not resonant with the cavity mode. To this end, in this paper, we write a closed expression for the coupling between an atom and the field within a cavity whose mirrors are dielectric multilayer stacks, which has only been reported in the case of single-layered dielectric mirrors.[22]

In order to model the dynamics within a cavity, the quantized light field is normalized in terms of its quantization volume, which usually corresponds to the geometric volume of the optical resonator.[23] However, in the case of the resonator considered, modeling the surface of the mirror as a hard boundary to the cavity mode is no longer appropriate. To rectify this, we consider an open cavity system, where the electric field is able to propagate through the dielectric mirror and couples to external free-space modes. This departs from the standard notion of having a mode volume and well defined frequency modes of the resonator, suitably modifying our calculation of the Purcell Factor. This goes substantially beyond the aspects that have been addressed before,[24,25] now taking into account a large number of dielectric layers and the off-resonant case, where the field and the design wavelength of the dielectric stacks are different.

We revise the concept of mode volume and cavity resonance for a cavity formed from dielectric mirrors and describe the general quantization procedure to be used for an atom within a cavity, where it interacts with a global electromagnetic field. This procedure departs from the standard input-output formulation used to model open optical systems.[23,26,27] A targeted application of this quantization model is the production of single photons leaking out from one side of the cavity. By applying the quantization procedure to a multilayer stack, we allow for a discussion on a more realistic specification of effective cavity length and corresponding mode volume for short cavities. We show that the expected resonance frequency of the cavity, the resonance frequency of the emitter, and the design frequency of the dielectric stack may differ substantially from one another. Finally, by considering the boundary to these effects, we demonstrate that the standard models of optical resonance are asymptotically re-achieved at extended cavity lengths.

We commence by characterizing the electromagnetic field within a cavity. Since the considered mirror structures are either flat or have large curvature radii, the field is described by its longitudinal propagation, in what is called the paraxial approximation.[13] Hence, for simplicity, we omit writing explicitly the transverse mode structure, any inclusion of which can be absorbed in the mode function obtained below. The solution for the longitudinal component is described by solving the Helmholtz equation

$$\left(\frac{d^2}{dx^2}+\epsilon_r(x)\frac{\omega^2}{c^2}\right)\Phi_\omega(x)=0, \tag{1}$$

where $\varepsilon_r(x)$ is the relative permittivity of the physical medium, $\Phi_\omega(x)$ is the space-dependent field eigenmode of continuous index $\omega = 2\pi c/\lambda$, λ is the wavelength of the traveling wave, and c is the speed of light. The corresponding quantized electric field can be written in the Schrödinger picture as

$$\hat{E}(x) = -i\int_0^\infty d\omega\sqrt{\frac{\hbar\omega}{2\varepsilon_0}}\left(\Phi_\omega(x)\hat{a}_\omega - \Phi^*_\omega(x)\hat{a}^\dagger_\omega\right). \tag{2}$$

We can write the general electromagnetic field as a sum of terms within, through, and outside the mirrors, $\Phi_\omega(x) = \Phi_{\omega,\mathrm{in}}(x) + \Phi_{\omega,\mathrm{stack}}(x) + \Phi_{\omega,\mathrm{out}}(x)$. The quantization procedure is performed in the whole universe, unlike any approaches first quantizing the field inside a perfect cavity and subsequently coupling the field modes to the outside using input-output formalisms.[26,27]

After the global field has been quantized, the Hamiltonian to include the atom within the cavity: Consider a point-like two-level atom with states $|g\rangle$ and $|e\rangle$ separated in energy by $\hbar\omega_A$, is positioned at $x = x_A$, between a perfect, mirror placed at $x = -\ell_c$ and a partially transparent dielectric mirror positioned at the origin. Here, $-\ell_c < x_A < 0$, where ℓ_c is the geometric length of the cavity. The electric field at the position of the atom can be written by evaluating Eq. (2) at $x = x_A$, and we consider a field-atom dipolar interaction $\hat{V} = -\hat{d}\hat{E}(x_A)$, where $\hat{d} = d\hat{\sigma}_+ + d^*\hat{\sigma}_-$ is the dipole operator of the atom, $\hat{\sigma}_+ = |e\rangle\langle g|$, and $\hat{\sigma}_- = |g\rangle\langle e|$.

The total Hamiltonian of the described system in rotating wave approximation is

$$\hat{H} = \hbar\omega_A\hat{\sigma}_+\hat{\sigma}_- + \int_0^{+\infty} d\omega\,\hbar\omega\,\hat{a}^\dagger_\omega\hat{a}_\omega + i\hbar\int_0^{+\infty} d\omega(\eta_\omega\hat{\sigma}_+\hat{a}_\omega - \eta^*_\omega\hat{a}^\dagger_\omega\hat{\sigma}_-), \tag{3}$$

where the first two terms correspond to the atom and electromagnetic field energy, and the third term to the interaction of said field with the atom placed between the mirrors. Additionally, the light-matter coupling η_ω is described by

$$\eta_\omega = \sqrt{\frac{\omega}{2\hbar\varepsilon_0}}\,d\,\Phi_{\omega,\mathrm{in}}(x_A). \tag{4}$$

For a passive (non-dispersive and non-dissipative) system, one can equivalently express the coupling term using Green functions, solutions of the Helmholtz equation with a Dirac-delta function as a source.[28,29]

To describe the dynamics of the open atom-cavity system accurately, an effective atom-cavity coupling strength needs to take into account the structure of the partially transparent mirror. A multilayered mirror consists of an alternating stack of two dielectric materials: The first type of layer has a width δ with refractive index n_1, while the second one has a width α with index n_2. The stack has $2N-1$ layers: $N-1$ pairs of dielectric and one additional layer of index n_1. As such,

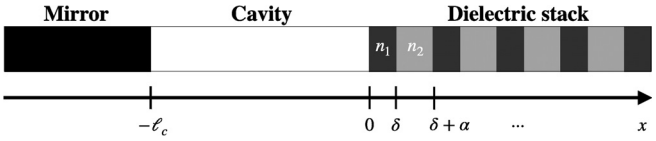

FIG. 1. Illustration of the considered cavity: a perfect mirror stands at $x = -\ell_c$, delimiting a cavity of geometric length ℓ_c with an alternating dielectric stack standing from zero.

the first and last layers of the stack have the higher refractive index[30] ($n_1 > n_2$). For the sake of simplicity, we disregard the substrate on which the coating is deposited. This model is shown in Fig. 1, having a relative permittivity given by

$$\varepsilon_r(x) = \begin{cases} 1, & -\ell_c < x \le 0, \\ n_1^2, & j_1(\delta+\alpha) < x \le j_1(\delta+\alpha)+\delta, \\ n_2^2, & (j_2-1)(\delta+\alpha)+\delta < x \le j_2(\delta+\alpha), \\ 1, & x > N(\delta+\alpha)-\alpha, \end{cases} \tag{5}$$

where $j_1 \in \{0, 1, 2, \ldots, N-1\}$ and $j_2 \in \{1, 2, \ldots, N-1\}$. The mirror is designed to reflect best at λ_0, which is used to specify the quarter wave dielectric optical thickness: $\delta = \lambda_0/4n_1$ and $\alpha = \lambda_0/4n_2$. For simplicity, we set $n_2 = 1$. In every region, Helmholtz's equation is solved by a superposition of plane waves,

$$\Phi_\omega(x) = A_+ e^{i\frac{\omega}{c}\sqrt{\epsilon_r(x)}x} + A_- e^{-i\frac{\omega}{c}\sqrt{\epsilon_r(x)}x}. \tag{6}$$

The distinct solutions are connected by the condition that $\Phi_\omega(x)$ and $d\Phi_\omega(x)/dx$ ensure continuity throughout the discontinuities of $\epsilon_r(x)$, fixing the values of A_+ and A_- for every region. The complete expression for the electromagnetic field is given by

$$\Phi_\omega(x) = \sum_{j=0}^{2N} C A_j(\omega, x)\chi_{\Omega_j}, \tag{7}$$

where j runs over the $2N-1$ possible layers, labeled $\Omega_j \subset \mathbb{R}$. $\chi_{\mathscr{D}}$ represents the indicator function $\chi_{\mathscr{D}}(x) = 1$ for $x \in \mathscr{D} \subset \mathbb{R}$ and 0 otherwise. The $2N$th term describes the mode exiting the cavity. C is a common normalization factor, and $A_j(\omega, x)$ corresponds to terms of the form of Eq. (6) with adequately chosen coefficients.

The solutions are shown in Fig. 2, and the analytic expression for the coefficients of each layer is shown in the supplementary material.

After the modes have been described in the form of Eq. (7), we consider the effective optical response of the structure. Following the normalization of the modes in Eq. (7), the inside and outside modes have the form

$$\Phi_{\omega,\text{in}}(x) = \frac{2i}{\sqrt{2\pi c\mathscr{A}}} e^{i\frac{\omega}{c}\ell_c}\mathscr{T}(\omega)\sin\left[\frac{\omega}{c}(x+\ell_c)\right], \tag{8}$$

$$\Phi_{\omega,\text{out}}(x) = \frac{1}{\sqrt{2\pi c\mathscr{A}}}\left(e^{2i\frac{\omega}{c}\ell_c}\frac{\mathscr{T}(\omega)}{\mathscr{T}^*(\omega)}e^{i\frac{\omega}{c}x} - e^{-i\frac{\omega}{c}x}\right), \tag{9}$$

where $\mathscr{A}$ is the transverse area of the mode (a quantity which is calculated when the mode is normalized in three dimensions). Here, $\mathscr{T}(\omega)$ is the field amplitude ratio of the structure, which has the form

$$\mathscr{T}(\omega) = \frac{e^{-i\frac{\omega}{c}(\ell_c+(N-1)(\delta+\alpha))}}{B^*_{2N-2}(\omega)}\frac{t(\omega)}{1+e^{i\frac{\omega}{c}\delta}e^{i\phi_B(\omega)}r(\omega)}, \tag{10}$$

where $\phi_B(\omega) = \arg(B_{2N-2}/B^*_{2N-2})$, and the single-layer spectral transmission response functions $t(\omega)$ and $r(\omega)$ are defined[23]

$$t(\omega) = \frac{(1-r_1^2)e^{i(n_1-1)\frac{\omega}{c}\delta}}{1-e^{2in_1\frac{\omega}{c}\delta}r_1^2}, \tag{11}$$

$$r(\omega) = e^{-i\frac{\omega}{c}\delta}\frac{r_1\left(e^{2in_1\frac{\omega}{c}\delta}-1\right)}{1-e^{2in_1\frac{\omega}{c}\delta}r_1^2} = |r(\omega)|e^{i\phi_r(\omega)}, \tag{12}$$

where r_1 is the single-layer reflectivity. Figure 3 shows a series of different cavity response functions for different numbers of layer stacks and cavity lengths. Our model exhibits the standard behavior of an optical cavity since an increase in the number of layers decreases the linewidth, as expected from an increased mirror reflectivity. Furthermore, the free spectral range of the cavity decreases as its length is increased.

As in single-layered cavities (see the details in the supplementary material), we can decompose $|\mathscr{T}(\omega)|^2$ as a sum of Lorentzian-like functions,

$$|\mathscr{T}(\omega)|^2 = \sum_{m=-\infty}^{\infty}\left(\frac{c}{\delta|B_{2N-2}(\omega)|^2}\times\frac{\gamma_N(\omega)}{(\omega-\tilde{\omega}_m(\omega))^2+\left(\frac{\gamma_N(\omega)}{2}\right)^2}\right), \tag{13}$$

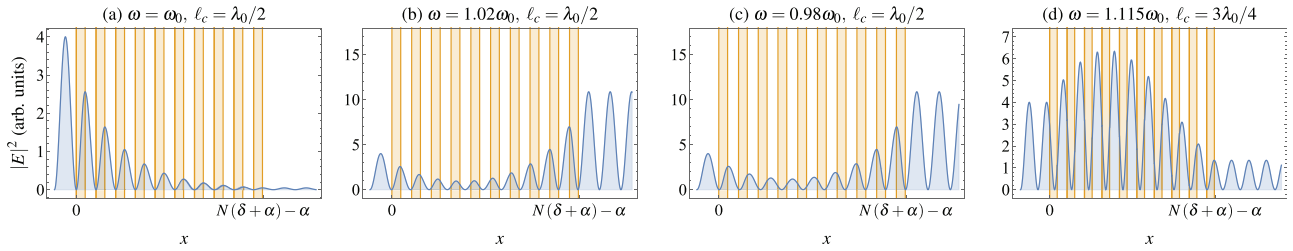

FIG. 2. Mode propagation of a wave of wavelength λ for a stack with $n_1 = 1.25$. A perfect mirror stands at $x = -\ell_c$, forming a cavity of length ℓ_c with a stack of 21 alternating layers of width $\delta = \lambda_0/4n_1$ and $\alpha = \lambda_0/4n_2$ (here, $n_2 = 1$). The propagation frequency $\omega = 2\pi c/\lambda$ is varied. In (a), the case when $\ell_c = \lambda_0/2$ and ω exactly matches with the cavity design resonance frequency ω_0 is shown, obtaining the strongest confinement of light inside of the cavity. In (b) and (c), the intensity changes when the propagating light is slightly off resonance. Finally, in (d) we set $\ell_c = 3\lambda_0/4$ and achieve resonance coupling when $\omega = 1.115\omega_0$. Moreover, in this case, the field intensity within the stack exceeds the intensity inside of the cavity.

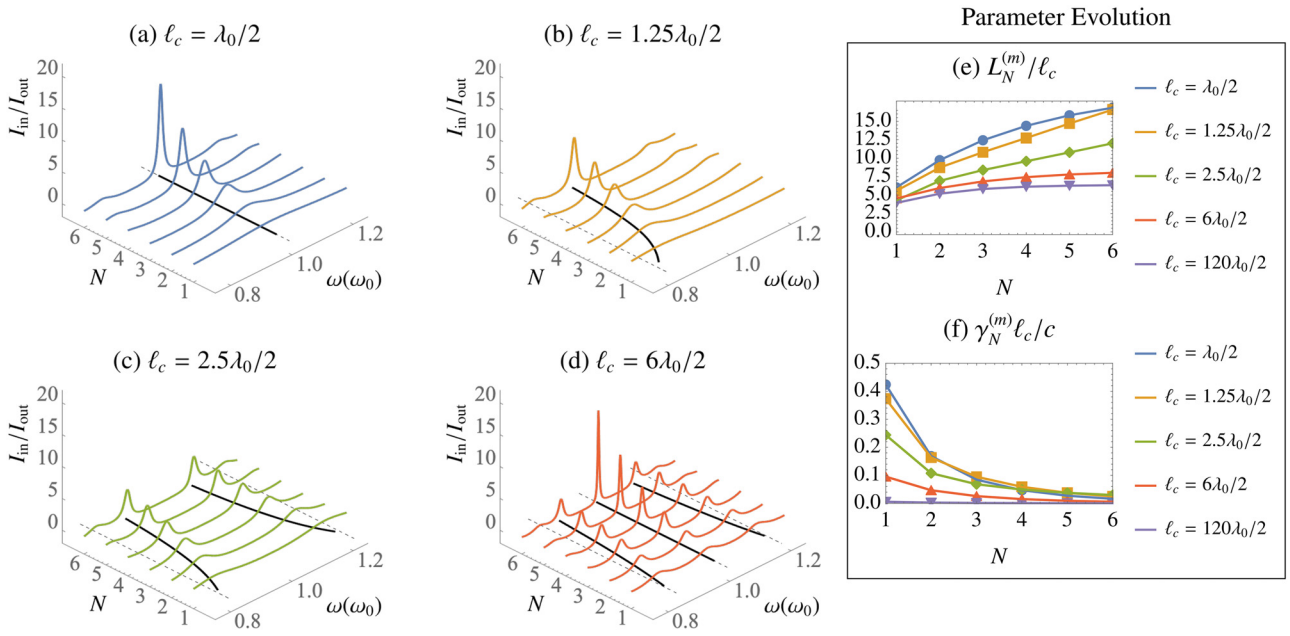

FIG. 3. Inside-outside intensity ratio, I_{in}/I_{out}, as a function of the angular frequency of the light and the number of layers, $2N-1$. The parameters of the cavity are as in Fig. 2. (a) shows $\ell_c = \lambda_0/2$, (b) $\ell_c = 1.25\lambda_0/2$, (c) $\ell_c = 2.5\lambda_0/2$, and (d) $\ell_c = 6\lambda_0/2$. All curves can be decomposed as sums of Lorentzian functions in ω. The dashed lines correspond to cavity classical resonances: $\omega_m = m\pi c/\ell_c$, where m is the number of antinodes between the mirrors. The black, solid lines correspond to $\omega_N^{(m)}$, the peak responses followed by the modes. These do not coincide with ω_m and are strongly dependent on the number of layers. (e) and (f) show the values of $L_N^{(m)}$ and $\gamma_N^{(m)}$ as a function of the layer number N for different values of ℓ_c.

where

$$\gamma_N(\omega) = -c\frac{\ln|r(\omega)|}{\delta/2}, \tag{14}$$

$$\tilde{\omega}_m = \frac{c\pi}{\delta/2}m - c\frac{(\phi_r(\omega)+\phi_B(\omega)+\pi)}{\delta}. \tag{15}$$

The term $\phi_B(\omega)$ in Eq. (15) accounts for the multilayer nature of the mirror. In the single-layered case, this has the form $\phi_{B_1}(\omega) = 2\ell_c\omega/c$.

Figure 3 implies that the multilayer structure leads to a narrowly peaked Lorentzian response function. In order to obtain the individual Lorentzians corresponding to each peak in the response function, we fit each individual peak to the exact cavity response function shown in Eq. (13), obtaining numerical values of $L_N^{(m)}$, $\gamma_N^{(m)}$, and $\omega_N^{(m)}$,

$$|\mathcal{T}(\omega)|^2 = \sum_m \frac{c}{2L_N^{(m)}}\frac{\gamma_N^{(m)}}{\left(\omega-\omega_N^{(m)}\right)^2+\left(\frac{\gamma_N^{(m)}}{2}\right)^2}. \tag{16}$$

We now examine what happens when we vary the spacing between the mirrors. By taking into account the multilayer structure of the mirror, we also observe resonance frequency shifts from the expected resonances, i.e., for a cavity having a mirror spacing ℓ_c, the expected resonance frequency would be $\omega_m = 2\pi c/\lambda_m = \pi m(c/\ell_c)$, where m is the number of antinodes between the mirrors. However, the resonance frequencies that we obtain with a multilayered structure, in general, do not match the values of ω_m described above (see Fig. 4). In other words, if in the multilayered case we write $\omega_{\text{eff}} = \omega_N^{(m)} = \pi m(c/\ell_{\text{eff}})$ for the resonance frequencies, then, in general, ℓ_{eff} is different from ℓ_c. In particular, ℓ_{eff} is the same as ℓ_c only if $\ell_c = p\lambda_0/2$, where $p \in \mathbb{Z}$. Moreover, the shorter the cavity, the greater the difference between ω_{eff} and ω_m.

Each term in Eq. (16) corresponds to a well separated single Lorentzian at a resonance frequency $\omega_N^{(m)}$, hence for the response function, we can write $\mathcal{T}(\omega) \approx \sum_m \mathcal{T}_m(\omega)$, where

$$\mathcal{T}_m(\omega) = \sqrt{\frac{c}{2L_N^{(m)}}}\frac{\sqrt{\gamma_N^{(m)}}}{\left(\omega-\omega_N^{(m)}\right)+i\frac{\gamma_N^{(m)}}{2}}. \tag{17}$$

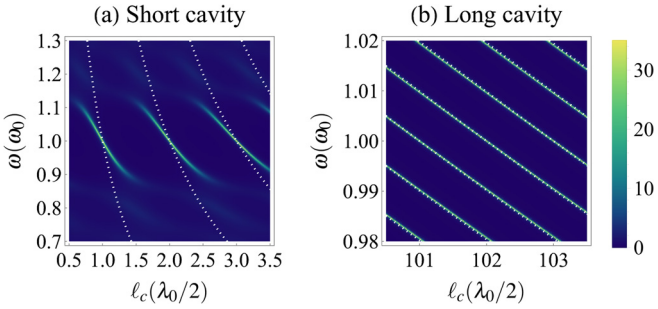

FIG. 4. Calculated inside/outside intensity ratio using the electromagnetic propagation of the mode vs $\pi mc/\ell_c$ shown in dotted lines. With very short cavities, the mismatch is appreciable and the maximum inside/outside ratio lines predicted classically differ significantly with respect to the mode prediction. The predicted and actual lines only match when $\ell_c = p\lambda_0/2$, for $p \in \mathbb{Z}$.

This expression for the response function is general; being applicable to cavities of any length, dielectric layer number, and refractive index n_1, and leads to the description of a general coupling strength $\eta_\omega = \sum_{m=-\infty}^{\infty} \eta_{\omega,m} = \sum_{m=-\infty}^{\infty} \xi_{\omega,m}\zeta_{\omega,m}$, where

$$\xi_{\omega,m} = i\sqrt{\frac{\omega}{\hbar\epsilon_0 L_N^{(m)}\mathscr{A}}}d, \tag{18}$$

$$\zeta_{\omega,m} = e^{i\frac{\omega}{c}\ell_c}\sin\left[\frac{\omega}{c}(x_A+\ell_c)\right]\sqrt{\frac{\gamma_N^{(m)}}{2\pi}}\frac{1}{\left(\omega-\omega_N^{(m)}\right)+i\frac{\gamma_N^{(m)}}{2}}. \tag{19}$$

We highlight that taking into account the transverse features (atom off-axis or higher-order modes) would simply result in the reduction of this coupling factor by a scalar.

Comparing this result with the single-layer case shown in the supplementary material, we can see that the expressions are the same, with the exception that for the multilayer case we have $L_N^{(m)}$ instead of ℓ_c and $\gamma_N^{(m)}$ instead of Γ_m. Similarly, if we interpret the product $L_N^{(m)}.\mathscr{A}$ in the pre-factor as the effective mode volume, it is no longer defined through the geometric length of the cavity, due to the discrepancy between $L_N^{(m)}$ and ℓ_c.

Over the width $\gamma_N^{(m)}$ of a single Lorentzian, ω is close to $\omega_N^{(m)}$ and varies very slowly; therefore we can further approximate the mode selective coupling: $\eta_{\omega,m} \approx \xi_{\omega_N^{(m)},m}\zeta_{\omega,m}$.

Previously, we presented a Hamiltonian describing the global closed system consisting of atom, cavity, and environment [Eq. (3)]. We now intend to extract an effective Hamiltonian to describe the dynamics of the open atom-cavity system. This extraction has been studied in the literature for the single-layer case.[26]

Given that the quantum information processing, retrieval, and storage of single photons all happen within the limited scenario of a single excitation within the cavity,[2] we limit the Hilbert space to a subspace containing the excited atom state $|e,0\rangle$ and the single excitation of the cavity in a superposition of frequency modes around the resonance frequency $\omega_N^{(m)}$: $|g,1_m\rangle$. To write the effective Hamiltonian for such a system, we define the operator

$$\hat{a}_m = \frac{1}{g_m}\int_0^\infty d\omega\,\eta_{\omega,m}\,\hat{a}_\omega, \tag{20}$$

satisfying the commutation relations $[\hat{a}_m, \hat{a}_{m'}^\dagger] = \delta_{mm'}$, $[\hat{a}_m, \hat{a}_{m'}] = 0$. The definition in Eq. (20) allows one to transform the continuous model (3) into a discrete one, and to define the single photon excitation around the resonance frequency $\omega_N^{(m)}$ as $|1_m\rangle = \hat{a}_m^\dagger|\mathbf{0}\rangle$.

It can be shown that g_m is a normalization constant given by (see the supplementary material)

$$g_m = i\sqrt{\frac{\omega_N^{(m)}}{\hbar\epsilon_0 L_N^{(m)}\mathscr{A}}}d\,e^{i\frac{\omega_N^{(m)}}{c}\ell_c}\sin\left[\frac{\omega_N^{(m)}}{c}(x_A+\ell_c)\right] + \mathcal{O}(\epsilon^2) \tag{21}$$

up to an error of the order ϵ^2, where $\epsilon = \gamma_N^{(m)}\frac{x_A+\ell_c}{c}$. The width $\gamma_N^{(m)}$ decreases with a greater number of layers and cavity length, hence ϵ becomes smaller (see Fig. 3) and the approximation is well validated.

Assuming that only one of the cavity modes at $\omega_N^{(m)}$ is close to the resonance frequency ω_A of the atom, all other modes can be safely disregarded and the effective Hamiltonian then reads (see the supplementary material)

$$\hat{H}_{\text{eff}} = \hbar\omega_A\hat{\sigma}_+\hat{\sigma}_- + \left(\hbar\omega_N^{(m)} - i\hbar\frac{\gamma_N^{(m)}}{2}\right)\hat{a}_m^\dagger a_m + i\hbar g_m\hat{\sigma}_+\hat{a}_m - i\hbar g_m^*\hat{\sigma}_-\hat{a}_m^\dagger, \tag{22}$$

where $\omega_N^{(m)} - \omega_A \ll \omega_N^{(m)}$, g_m is the coupling of a single cavity mode $\omega_N^{(m)}$ with the atom, and $\gamma_N^{(m)}$ is the width of Lorentzian centered at the resonance frequency $\omega_N^{(m)}$.

Equation (21) has the form of the atom-cavity coupling for a perfect cavity [see the supplementary material, Eq. (S73)], with a corrected geometric cavity length and resonance frequency.

In conclusion, analyzing the multilayer structure enabled a more realistic description of the effective cavity length and corresponding mode volume. The effective cavity length ℓ_{eff}, as defined in the literature,[16,31,32] determines the cavity resonance and, as we have shown, does not correspond to the coupling factor cavity length $L_N^{(m)}$ used for determining the cavity-matter coupling. We have found that these two lengths are not necessarily equal when considering a multilayer structure. Additionally, the resonance frequencies defining ℓ_{eff} no longer coincide with the expected resonances at integer multiples of $c/(2l_c)$. A pronounced consequence of this discrepancy is that the most common approach[13] for determining a cavity length by means of measuring its free-spectral range is bound to fail for very short cavities. The geometric length of the cavity might differ by up to $\lambda_0/2$ from the effective length determining the free spectral range.

Additionally, we have explicitly calculated the atom-cavity coupling rate both for on and off resonant behavior from an open-system Hamiltonian calculated from the general quantized field. This quantization from first principles of more realistic open cavities is a preliminary step for considering complex dynamics that feature laser driving. Work is ongoing to derive microscopic models[33] for controlling photonic states produced from such cavities.[7]

We also note that submicrometric confinement of light in (dissipative and dispersive) metallic media gives rise to surface plasmon polaritons that can be used for quantum optics at nanoscale.[34] Albeit these are no multilayered structures, the construction of quantized models taking into account the resulting losses follows a similar approach and is based on a microscopic oscillator model for the medium coupled to the electromagnetic field[35] with a particular care for finite-size media.[36,37]

The model introduced here will be useful to describe the leakage of single photons from the cavity to the environment. This is relevant when using emitters inside of short cavities, where this effect is manifested. Some of the following are potential applications: coupling of ions[18] and atoms to fiber-tip optical cavities,[38] quantum dots,[39] the use of two different frequencies within a short multilayered cavity,[40] NV centers[9,15,41] (where the mode structure and more-resonances have been studied in fiber-tip cavities[42]) and, in general, whenever there is a very short cavity that couples strongly to a discrete quantum emitter. In many cases, the substantial deviations from the simple model discussed would make it impossible to establish strong coupling unless these corrections were considered. These results could also prove useful for the spectral characterization of devices with multilayered structures.[43]

See the supplementary material for a derivation of the physical properties of the single-layer model, the analytical formulas for the

modes shown in Fig. 2, a description of the Lorentzian structure of the cavity response function, and a derivation of the Hamiltonian in Eq. (22).

J.R.A. acknowledges Christian Poveda regarding code optimization. All authors acknowledge Mark IJspeert, Marwan Mohammed, Ezra Kassa, and Hans-Rudolf Jauslin for useful discussions.

This work has received funding from European Union Horizon 2020 (Marie Sklodowska-Curie 765075-LIMQUET), EPSRC through the quantum technologies program (NQIT hub, No. EP/M013243/1), and EIPHI Graduate School (No. ANR-17-EURE-0002).

DATA AVAILABILITY

The data that support the findings of this study are openly available in the Oxford University Research Archive at https://doi.org/10.5287/bodleian:dq9jJPxG5, Ref. 44.

REFERENCES

[1]J. I. Cirac and H. J. Kimble, Nat. Photonics **11**, 18 (2017).
[2]S. Ritter, C. Nölleke, C. Hahn, A. Reiserer, A. Neuzner, M. Uphoff, M. Mücke, E. Figueroa, J. Bochmann, and G. Rempe, Nature **484**, 195 (2012).
[3]H. J. Kimble, Nature **453**, 1023 (2008).
[4]T. Wilk, S. C. Webster, A. Kuhn, and G. Rempe, Science **317**, 488 (2007).
[5]D. L. Moehring, P. Maunz, S. Olmschenk, K. C. Younge, D. N. Matsukevich, L.-M. Duan, and C. Monroe, Nature **449**, 68 (2007).
[6]T. D. Barrett, A. Rubenok, D. Stuart, O. Barter, A. Holleczek, J. Dilley, P. B. R. Nisbet-Jones, K. Poulios, G. D. Marshall, J. L. O'Brien *et al.*, Quantum Sci. Technol. **4**, 025008 (2019).
[7]A. Kuhn, M. Hennrich, T. Bondo, and G. Rempe, Appl. Phys. B **69**, 373 (1999).
[8]M. Keller, B. Lange, K. Hayasaka, W. Lange, and H. Walther, Nature **431**, 1075 (2004).
[9]S. Johnson, P. R. Dolan, T. Grange, A. A. P. Trichet, G. Hornecker, Y. C. Chen, L. Weng, G. M. Hughes, A. A. R. Watt, A. Auffèves *et al.*, New J. Phys. **17**, 122003 (2015).
[10]X. Ding, Y. He, Z.-C. Duan, N. Gregersen, M.-C. Chen, S. Unsleber, S. Maier, C. Schneider, M. Kamp, S. Höfling *et al.*, Phys. Rev. Lett. **116**, 020401 (2016).
[11]E. Purcell, Phys. Rev. **69**, 37–38 (1946).
[12]H. J. Kimble, Phys. Scr. **1998**, 127.
[13]B. E. Saleh and M. C. Teich, *Fundamentals of Photonics* (John Wiley & Sons, 1991), Vol. 22.
[14]H. A. Macleod, *Thin-Film Optical Filters* (Institute of Physics Publishing, 2018), ISBN: 978-1-315-27049-4 978-1-351-98222-1.
[15]A. M. Kern, D. Zhang, M. Brecht, A. I. Chizhik, A. V. Failla, F. Wackenhut, and A. J. Meixner, Chem. Soc. Rev. **43**, 1263 (2014).
[16]P. Zhong, W. Rong-han, and W. Qi-ming, Acta Phys. Sin. (Overseas Ed.) **4**, 810 (1995).
[17]J. H. Apfel, Appl. Opt. **16**, 1880 (1977).
[18]K. J. Vahala, Nature **424**, 839 (2003).
[19]P. T. Kristensen, C. V. Vlack, and S. Hughes, Opt. Lett. **37**, 1649 (2012).
[20]P. T. Kristensen and S. Hughes, ACS Photonics **1**, 2 (2014).
[21]C. Sauvan, J. P. Hugonin, I. S. Maksymov, and P. Lalanne, Phys. Rev. Lett. **110**, 237401 (2013).
[22]S. M. Dutra and P. L. Knight, Phys. Rev. A **53**, 3587 (1996).
[23]W. Vogel and D.-G. Welsch, *Quantum Optics*, 1st ed. (Wiley, 2006), ISBN: 978-3-527-40507-7 978-3-527-60852-2.
[24]K. Ujihara, A. Nakamura, O. Manba, and X.-P. Feng, Jpn. J. Appl. Phys. **30**, 3388 (1991).
[25]X.-P. Feng, Opt. Commun. **83**, 162 (1991).
[26]S. M. Dutra, *Cavity Quantum Electrodynamics: The Strange Theory of Light in a Box*, Wiley Series in Lasers and Applications (Wiley, Hoboken, NJ, 2005), ISBN: 978-0-471-44338-4.
[27]D. Walls and G. J. Milburn, in *Quantum Optics*, edited by D. Walls and G. J. Milburn (Springer, Berlin, 2008), pp. 127–141, ISBN: 978-3-540-28574-8.
[28]M. Wubs, L. G. Suttorp, and A. Lagendijk, Phys. Rev. A **70**, 053823 (2004).
[29]M. V. Rybin, S. F. Mingaleev, M. F. Limonov, and Y. S. Kivshar, Sci. Rep. **6**, 20599 (2016).
[30]M. Banning, J. Opt. Soc. Am. **37**, 792 (1947).
[31]Y. Suematsu, S. Arai, and K. Kishino, J. Lightwave Technol. **1**, 161 (1983).
[32]L. A. Coldren, S. W. Corzine, and M. L. Mashanovitch, *Diode Lasers and Photonic Integrated Circuits*, 2nd ed. (Wiley-Blackwell, Hoboken, NJ, 2012), ISBN: 978-0-470-48412-8.
[33]G. L. Giorgi, A. Saharyan, S. Guérin, D. Sugny, and B. Bellomo, Phys. Rev. A **101**, 012122 (2020).
[34]D. E. Chang, A. S. Sørensen, E. A. Demler, and M. D. Lukin, Nat. Phys. **3**, 807 (2007).
[35]B. Huttner and S. M. Barnett, Phys. Rev. A **46**, 4306 (1992).
[36]V. Dorier, J. Lampart, S. Guérin, and H. R. Jauslin, Phys. Rev. A **100**, 042111 (2019).
[37]V. Dorier, S. Guérin, and H.-R. Jauslin, Nanophotonics **9**, 3899 (2020).
[38]M. Brekenfeld, D. Niemietz, J. D. Christesen, and G. Rempe, Nat. Phys. **16**, 647 (2020).
[39]V. Loo, L. Lanco, A. Lemaître, I. Sagnes, O. Krebs, P. Voisin, and P. Senellart, Appl. Phys. Lett. **97**, 241110 (2010).
[40]S. Garcia, F. Ferri, J. Reichel, and R. Long, Opt. Express **28**, 15515 (2020).
[41]A. A. P. Trichet, P. R. Dolan, D. James, G. M. Hughes, C. Vallance, and J. M. Smith, Nano Lett. **16**, 6172 (2016).
[42]E. Janitz, M. Ruf, M. Dimock, A. Bourassa, J. Sankey, and L. Childress, Phys. Rev. A **92**, 043844 (2015).
[43]C. J. Hood, H. J. Kimble, and J. Ye, Phys. Rev. A **64**, 033804 (2001).
[44]A. Saharyan, J. Alvarez Velasquez, T. Doherty, A. Kuhn, and S. Guerin (2021). "Light-matter interaction in open cavities with dielectric stacks," Oxford University Research Archive. https://doi.org/10.5287/bodleian:dq9jJPxG5